Cellular/Molecular

Developmental Control of Synaptic Receptivity

Alison J. Barker,[1,2] Selina M. Koch,[1,2,3] Jamian Reed,[1,2] Ben A. Barres,[4] and Erik M. Ullian[1,2,3]

Departments of [1]Ophthalmology and [2]Physiology and [3]Neuroscience Graduate Program, University of California, San Francisco, San Francisco, California 94143-0730, and [4]Department of Neurobiology, Stanford University School of Medicine, Stanford, California 94305-5125

Are neurons born with the ability to form and receive synapses or do they acquire these abilities during development? We have previously found that purified postnatal retinal ganglion cells (RGCs) require soluble astrocyte-derived signals to form synapses *in vitro* and *in vivo*. Here we show that newly generated embryonic day 17 (E17) RGCs are able to form but not receive synapses under these conditions. Dendrite growth is not sufficient to trigger receptivity; rather, the ability of newly generated RGCs to receive synapses is acquired at E19 in response to direct contact by neighboring cell types. Direct contact with astrocytes, which are not present at E17 but are normally generated by E19, is sufficient to induce synaptic receptivity in E17 RGCs. In contrast, amacrine contact does not induce synaptic receptivity. Interestingly, astrocyte contact alters the localization of the synaptic adhesion molecule neurexin away from dendrites. In addition, dendritic expression of neurexin is sufficient to prevent astrocyte contact-mediated increases in synapse number, suggesting a molecular mechanism by which astrocyte contact regulates neuronal synaptic receptivity. Thus, synaptic receptivity is not induced simply by dendritic elaboration but must be signaled by both contact-mediated signaling from astrocytes and a shift in the dendritic localization of neurexin.

Key words: **synaptogenesis; retinal ganglion cells (RGCs); astrocytes; glia; dendrite arborization; rat**

Introduction

Significant advances have been made in our understanding of the molecular mechanisms of synaptogenesis, yet we still understand little about how the number of synapses a neuron makes or receives is regulated both temporally and spatially. For example, is synapse number an intrinsic property of a neuron or is it largely controlled by extrinsic signals? And when do embryonic neurons turn on their developmental program or become receptive to extrinsic signals? Recent studies of purified neurons show that synapse number can be controlled by extrinsic signals. Retinal ganglion cells (RGCs) purified away from all other retinal cell types are unable to effectively form synapses unless cocultured with astrocytes, which provide soluble signals such as thrombospondin (TSP), which strongly enhance the number of synapses these neurons can make (Mauch et al., 2001; Nägler et al., 2001; Ullian et al., 2001; Christopherson et al., 2005). Similarly, purified spinal motor neurons also depend on extrinsic signals provided by astrocytes or Schwann cells to form synapses *in vitro* (Ullian et al., 2004a). These studies provide evidence that extracellular signals from non-neuronal cell types can powerfully control synaptogenesis and raise the question of whether newly generated neurons are intrinsically capable of synaptogenesis. The possibility that either intrinsic or extrinsic developmental programs help to regulate the timing, location, or number of newly forming synapses has received relatively little consideration.

Although it is generally assumed that neurons are generated with the ability to both form and receive synapses, a previous study found that embryonic hippocampal neurons are capable of forming but not receiving synapses. These cultured embryonic neurons acquire synaptic receptivity at the same time that their dendritic arbors begin to elaborate. Although the timing of these events suggests that synaptic receptivity is controlled by the amount of dendritic area available to receive synaptic inputs (Fletcher et al., 1994), it does not preclude the possibility that there are two distinct mechanisms, one controlling dendrite elaboration and a second controlling synaptic receptivity.

Here we have taken advantage of our methods to highly purify and culture rodent retinal ganglion cells (>99% purity) to investigate when and how synaptic receptivity is acquired during normal development. RGCs purified from embryonic day 17 (E17) are unable to receive many synapses, even when they have extended long dendrites, and even though they are able to form synapses on more mature postnatal RGCs. Purified E17 RGCs do not acquire the ability to receive synapses with time in culture, indicating that synaptic receptivity is not acquired as the result of an intrinsic maturation program. RGCs in mixed retinal cultures or *in vivo* are fully able to receive synapses at E19. Significantly, E19 marks the first contacts between RGCs and various retinal cell types, strongly indicating that synaptic receptivity is induced by neighboring cell types.

Because RGCs establish contact with amacrine cells and astrocytes during embryonic development, we tested the hypothesis that contact with these cells is responsible for initiating synaptic receptivity. Coculture of purified E17 RGCs in contact with pu-

Received Dec. 4, 2006; revised June 19, 2008; accepted June 26, 2008.

This work was supported by a Zaffaroni Fellowship, the Sandler Family Fund, the Alfred P. Sloan Foundation, a March of Dimes Basil O'Connor Award, a Research to Prevent Blindness Young Investigator Award, the Autism Speaks Foundation, That Man May See (E.M.U.), National Institutes of Health–National Eye Institute Grant T32EY07120 (S.M.K.), and National Institute of Drug Addiction Grant DA15043 (B.A.B.). We thank Dr. Peter Scheiffele for anti-neurexin and neuroligin antibodies and neurexin-HA constructs.

Correspondence should be addressed to Erik M. Ullian, Department of Ophthalmology, University of California, San Francisco, 10 Koret Way, San Francisco, CA 94143-0730. E-mail: ulliane@vision.ucsf.edu.

DOI:10.1523/JNEUROSCI.1744-08.2008

 0270-6474/08/288150-11$15.00/0

rified astrocytes, but not with purified amacrine cells, is sufficient to induce synaptic receptivity. These findings show that developing RGCs are not born with the ability to receive synapses, but acquire it in response to contact-mediated signaling by neighboring cells.

Additionally, we report that concomitant with the induction of embryonic synaptic receptivity, astrocyte contact induces changes in the dendrite localization of the synaptic protein neurexin (NRX). In mammals, three neurexin genes have been identified, each with an α and shortened β form (Dean and Dresbach, 2006; Craig and Kang, 2007). Although neurexin is traditionally viewed as the presynaptic component of the neurexin–neuroligin (NLG) complex, recent evidence (Taniguchi et al., 2007) has shown endogenous levels of dendritic neurexin. Interestingly, this endogenous expression is postulated to play an inhibitory role in synapse formation. We found that embryonic neurons have significant neurexin localization to dendrites, and this localization is reversed by astrocyte contact, providing a possible mechanism by which developing neurons regulate the precise timing of synapse formation in response to contact with neighboring cell types. Importantly, we were able to show that overexpression of a single neurexin, neurexin1β, eliminated the astrocyte contact effect, providing support for an inhibitory role for neurexin in synapse formation.

Materials and Methods

Cell purification and culture. RGCs from postnatal day 5 (P5) or E17 albino rats (Simonsen rats; Simonsen Laboratories) were purified as described previously (Barres et al., 1988). Briefly, dissected retinas were enzymatically dissociated in papain in Dulbecco's PBS (DPBS; Invitrogen) to create a single-cell suspension. RGCs were isolated from this suspension using sequential immunopanning to >99.5% purity (Barres et al., 1988). Purified RGCs were plated on 12 mm glass coverslips (Carolina Science and Math) in 24-well tissue culture plates (BD Biosciences) at a density of 30,000 cells per coverslip (~26,000 cells/cm^2). Coverslips were pretreated for 30 min with poly-D-lysine (PDL; 70 kDa, 10 μg/ml; Sigma) at room temperature followed by overnight incubation with mouse laminin (Sigma).

RGCs were cultured in 500 μl of defined, serum-free medium, modified from Bottenstein et al. (1979). Media contained Neurobasal (Invitrogen), bovine serum albumin, selenium, putrescine, triiodothyronine, transferrin, progesterone, pyruvate (1 mM; Sigma), glutamine (2 mM; Sigma), ciliary neurotrophic factor (10 ng/ml; Regeneron Pharmaceuticals), brain-derived neurotrophic factor (50 ng/ml; Regeneron Pharmaceuticals), insulin (5 μg/ml; Sigma), and forskolin (10 μM; Sigma), as defined by Ullian et al. (2001). Cultures were maintained at 37°C in a humidified environment of 10% CO_2/90% O_2 (Praxair). Under these conditions, more than half of the RGCs survive *in vitro* for at least 1 month (Meyer-Franke et al., 1995).

Cortical astrocyte cultures were prepared from P1–P2 Sprague Dawley rats as described previously (McCarthy and de Vellis, 1980). Briefly, the cortex was dissected and digested in trypsin. Cells were plated in tissue culture flasks (BD Biosciences) in a medium that does not allow survival of neurons [DMEM, fetal bovine serum (10%), penicillin (100 U/ml), streptomycin (100 mg/ml), glutamine (2 mM), and Na-pyruvate (1 mM)]. After 4 d in culture, nonadherent cells were removed from flasks by shaking. Remaining cells were removed from flasks enzymatically and cultured on PDL (70 kDa, 10 μg/ml; Sigma)-coated tissue culture plates (BD Biosciences) in astrocyte growth medium (Ullian et al., 2001). Astrocyte cultures could be maintained for long-term culture by routinely passaging confluent cultures by enzymatically removing astrocytes from culture plates and replating them at lower density on new plates.

Optic nerve astrocytes were prepared as described previously (Mi and Barres, 1999). Briefly, optic nerves were dissected from P5 rats and dissociated in trypsin. The optic nerve astrocytes were specifically purified using a sequential immunopanning procedure for negative selection and Ran-2 for positive selection. Astrocytes were then trypsinized off of the final panning plate and plated onto PDL-coated coverslips.

Astrocytes were fixed with the addition of 100% methanol for 30 min at room temperature. Before plating RGCs in contact with fixed astrocytes, the fixed layers were rinsed three times with Dulbecco's PBS at 2 h intervals.

Labeling purified neurons. To specifically label either P5 or E17 neurons for heterochronic coculture experiments, neurons were incubated at 37°C in CT-Cell tracer dye (Invitrogen) for 15 min in Earle's balanced salt solution (EBSS). Dye containing EBSS was removed and replaced with full RGC growth media for an additional 30 min. Cells were then rinsed eight times with DPBS and trypsinized off the final panning plate.

Synaptic assay and immunocytochemistry. After treatment, cultures were fixed for 7 min at room temperature in 4% paraformaldehyde (PFA) prewarmed to 37°C. The PFA was then aspirated off, and cultures were washed three times with PBS. The coverslips were removed from the culture plate, and 100 μl of blocking buffer [50% antibody buffer (0.5% bovine serum albumin, 0.5% Triton X-100, 30 mM $NaPO_4$, pH 7.4, 750 mM NaCl, 5% normal goat serum (NGS), and 0.4% NaN_3), 50% goat serum, and 0.1% Triton X-100] was added for 30 min. After blocking, coverslips were washed three times in PBS. For staining of excitatory synapses, primary antibody solution contained monoclonal rabbit anti-rat synaptotagmin (cytosolic domain; Synaptic Systems) and monoclonal mouse anti-PSD-95 (6G6-1C9 clone; Affinity BioReagents) diluted 1:500. One hundred microliters of primary antibody solution were added to each coverslip. Coverslips were incubated overnight at 4°C. After incubation, coverslips were washed five times in PBS. Secondary antibody solution containing Alexa-594-conjugated goat anti-rabbit and Alexa-488-conjugated goat anti-mouse (Invitrogen) at a dilution of 1:500 in antibody buffer was added. Coverslips were incubated in secondary antibody solution for 2 h at room temperature. After incubation, coverslips were washed five times in PBS, then mounted in Vectashield mounting medium containing 4′,6′-diamidino-2-phenylindole (DAPI; a cellular nuclear marker) (Vector Laboratories) on glass slides (VWR Scientific). Mounted coverslips were stored at −30°C until used. Mounted coverslips were imaged using Nikon Diaphot and Eclipse epifluorescence microscopes. Healthy cells that were at least two cell diameters from their nearest neighbor were identified and selected at random by eye using DAPI fluorescence. Eight-bit digital images of the fluorescence emission at both 594 and 488 nm were obtained for each selected cell using a cooled monochrome CoolSnap camera and SPOT or Image Q, image capture software (Diagnostic Instruments). Each single-channel image was adjusted to remove unused portions of the pixel value range, and the used pixel values were adjusted appropriately to use the entire pixel value range. Corresponding channel images were then merged to create a color [RGB (red–green–blue)] image containing the two single-channel images as individual color channels, using a custom software package called SpotRemover (2001 Barry Wark) (Christopherson et al., 2005). On Macintosh OS X, these manipulations can be performed automatically.

Synapses were identified by colocalization (overlap) of synaptotagmin and PSD-95 puncta. Although presynaptic and postsynaptic sites do not actually overlap, the resolving power of light microscopy prevents distinguishing individual puncta at a single synapse. Colocalized puncta were identified and characterized using a custom written plug-in (2001 Barry Wark) (Christopherson et al., 2005) for the NIH image-processing package, ImageJ version 1.24 and greater (available at http://rsb.info.nih.gov/ij/). Full documentation of the punctum-counting algorithm is available in the "Puncta Analysis" plug-in's source code. Briefly, the rolling ball background subtraction algorithm was used to remove low-frequency background from each image channel. The user was then prompted to "mask" the puncta in the single-channel image by thresholding the image so that only puncta remained above threshold. ImageJ's "Particle Analyzer" plug-in was then used to identify and characterize puncta within each channel. Puncta in different color channels were defined as colocalized if the centers of two circles, centered at the puncta's centroids and with areas equal to the puncta's area, were less than the radius of the larger of the two circles apart. Number, mean area, mean minimum and maximum pixel intensities, and mean mean pixel intensities for all synaptotagmin, PSD-95, and colocalized puncta in the image were recorded

and saved to disk for later analysis. Data analysis, including ANOVA, was performed in SigmaStat (SPSS). Unless noted, ANOVA was performed using the Student–Newman–Keuls method, and ANOVA on ranks was performed using the Kruskal–Wallis method with Dunn's method of multiple comparison. Data visualization was completed in SigmaPlot (SPSS). All experiments were repeated three times with separate biological samples.

To characterize dendritic complexity, cultured E17 and P5 neurons (prepared for staining as detailed above) were immunostained with monoclonal mouse anti-MAP2 (Millipore Bioscience Research Reagents), a dendrite-specific marker. Images were visualized using Nikon 80i epifluorescence and captured with a cooled monochrome CoolSnap camera. Images were further analyzed by custom plug-ins for the NIH image-processing package, ImageJ (available at http://rsb.info.nih.gov/ij/). To analyze individual dendritic fields, single neurons were traced using NeuronJ (Meijering et al., 2004) (available at http://www.imagescience.org/meijering/software/neuronj/). Traced neurons were saved as 8 bit grayscale images and analyzed by a custom Sholl Analysis plug-in (available at http://www-biology.ucsd.edu/labs/ghosh/software/index.html). Radii for Sholl analysis were programmed to extend four cell body lengths from the soma, encompassing the same dendritic area used to quantify synapses (see above).

Immunohistochemistry. Whole heads from embryonic day 17 and 19 Sprague Dawley rats were fixed in 4% paraformaldehyde (in PBS) for 4 or 24 h (E17 and E19, respectively). Heads were cryoprotected in 30% sucrose in PBS. After cryoprotection, tissues were sectioned by freezing microtome into 0.75 μm sections in 0.1 M phosphate buffer. Sections were washed three times with PBS followed by 30 min room temperature (RT) blocking in 5% normal goat serum and 0.25% Triton X-100 in PBS (blocking buffer). Blocking was followed by a 1 h RT primary incubation using primary antibodies monoclonal mouse anti-GFAP (Millipore Bioscience Research Reagents; 1:500) to visualize astrocytes and monoclonal rabbit anti-neuronal class III β-tubulin (Covance; 1:500) in PBS as a neuronal marker. After primary incubation, sections were washed once with PBS. Secondary incubation with Alexa-594-conjugated goat anti-mouse and Alexa-488-conjugated goat anti-rabbit (Invitrogen) was performed at a 1:500 dilution in blocking buffer for 1 h at RT. After secondary incubation, sections were washed three times with PBS at RT and mounted using Vectashield with DAPI (Vector Laboratories) onto glass slides (VWR Scientific).

Whole eyes were rapidly excised and fixed in 4% paraformaldehyde in phosphate buffer for 15–30 min. Tissue was cryoprotected overnight at 4°C (30% sucrose in PBS). Sections (30 μm) were mounted directly onto Fisherbrand Superfrost microscope slides (Fisher Scientific). Blocking for 30 min at RT with blocking buffer was followed by an overnight primary incubation at 4°C in PBS, using monoclonal rabbit anti-neuronal class III β-tubulin (Covance) at a 1:1500 dilution to visualize neurons and monoclonal mouse anti-synaptic vesicle protein 2 (SV2) (Developmental Hybridoma Bank, University of Iowa) at a 1:100 dilution, as a presynaptic marker. Slides were washed in PBS and incubated for 3 h at RT with secondary antibodies Alexa-594-conjugated goat anti-rabbit and Alexa-488-conjugated goat anti-mouse (Invitrogen) diluted 1:1000 in blocking buffer. After secondary incubation, slides were washed three times with PBS and mounted using Vectashield with DAPI (Vector Laboratories) onto glass slides (VWR Scientific). Staining was visualized with a Nikon Eclipse 80i epifluorescence microscope.

Neurexin and neuroligin staining. E17 RGCs cultured with and without astrocyte contact for 7–10 d *in vitro* were stained for chicken anti-pan-neurexin (kind gift from P. Scheiffele, University of Basel, Basel, Switzerland; 1:200) or rabbit anti-pan-neurexin (Synaptic Systems; 1:500) and polyclonal rabbit anti-pan-neuroligin (kind gift from P. Scheiffele; 1:400). Coverslips stained for neuroligin were fixed with a combined PFA/methanol method. Briefly, cells were fixed with 4% paraformaldehyde solution for 10 min at RT, followed by a 2 min methanol permeabilization at RT. Coverslips were washed five times with PBS followed by a primary antibody incubation overnight at 4°C. Neuroligin secondary staining and neurexin staining were performed as detailed above (see Synaptic assay and immunocytochemistry). Intensity of neurexin staining was quantified using the NIH image-processing package, ImageJ. Equal-exposure images acquired using Simple PCI software (Compix) were converted to 8 bit grayscale images and background subtracted. Mean grayscale intensity measurements were made along a two-pixel-width line along 12.5 μm lengths of dendrite using the measurement tool option. This allowed for the measurement of intensity along the dendrite only.

Transient transfection. Embryonic RGCs were transiently transfected using the Effectene Cell Transfection Reagent (Qiagen) following the manufacturer's instructions. Hemagglutinin (HA)-tagged NRX constructs were generously provided by Dr. Peter Scheiffele [NRX1β4(−)-HA, as described by Taniguchi et al. (2007)]. After 10 d in culture, embryonic RGCs were fixed and processed for immunostaining as described above (see Synaptic assay and immunocytochemistry). Synaptic markers, synaptotagmin, and PSD-95 were used as presynaptic and postsynaptic markers, respectively (details provided above), and transfected neurons were visualized by immunostaining for the HA tag using chicken anti-HA (Millipore Bioscience Research Reagents) at a 1:250 dilution. Staining was visualized with a Nikon Eclipse 80i epifluorescence microscope.

Electrophysiology. Membrane currents were recorded using whole-cell patch-clamp techniques at a holding voltage of −70 mV as described previously (Ullian et al., 2001). Patch pipettes (3–5 MΩ) were pulled from borosilicate glass (World Precision Instruments). External solution contained (in mM) 120 NaCl, 3 $CaCl_2$, 2 $MgCl_2$, 5 KCl, and 10 HEPES, pH 7.3. Internal pipette solution contained (in mM) 100 K-gluconate, 10 KCl, 10 EGTA (Ca^{2+}-buffered to 10^{-6}), and 10 HEPES, pH 7.3. All experiments were performed at room temperature (18–22°C). Whole-cell currents were recorded using pClamp software for Windows (Molecular Devices). Miniature EPSCs (mEPSCs) and spontaneous EPSCs were recorded in the presence and absence of TTX (Alomone Labs), analyzed using Mini Analysis Program (SynaptoSoft), and plotted using SigmaPlot or Origin (Microcal).

Results

Purification of embryonic RGCs by immunopanning

To determine whether embryonic neurons are capable of making synapses *in vitro*, we purified embryonic retinal ganglion cells from a variety of ages using an immunopanning procedure we previously developed for purification of postnatal RGCs (Barres et al., 1988). The purity of the postnatal RGCs isolated using this method is >99.5%, as determined by retrograde labeling. Because retrograde labeling of embryonic RGCs cannot be used to confirm purity, we instead labeled immunopanned embryonic RGCs with early RGC-specific markers: β-tubulin and Brn3b (Watanabe et al., 1991; Liu et al., 2000). E17 retinal sections stained with an anti-β-tubulin antibody showed labeling of most cells in the ganglion cell layer (supplemental Fig. 1*A*, available at www.jneurosci.org as supplemental material), indicating its specificity at this age. We found that 100% of the neurons purified from E17 retina label with the anti-β-tubulin antibody, indicating that they are highly purified RGCs (supplemental Fig. 1*B*, available at www.jneurosci.org as supplemental material). Brn3b is a transcription factor expressed by most, but not all, RGCs as soon as they have differentiated (Liu et al., 2000). We found that anti-Brn3b-specific antibody labels cells predominantly in the RGC layer of the embryonic retina (supplemental Fig. 1*C*, available at www.jneurosci.org as supplemental material). Consistent with this conclusion, we detected Brn3b nuclear immunoreactivity in ~90% of the cells in our E17 RGC cultures (supplemental Fig. 1*D*, available at www.jneurosci.org as supplemental material), a percentage that is consistent with the percentage of RGCs in E17 retinal sections and purified postnatal RGCs that label with this antibody. In combination, these two antigenic markers were used to assess the purity of the putative purified population of RGCs we isolated from E17 retina by immunopanning (see Materials and Methods). In contrast, none of the puri-

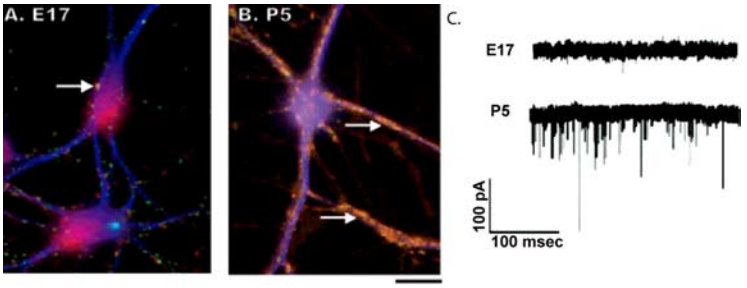

Figure 1. Examples of RGCs purified from E17 and P5 retina and stained for synaptic markers synaptotagmin (red) and PSD-95 (green) after 2 weeks in culture. ***A***, E17 RGCs with astrocyte feeding layers show few synaptic puncta and relatively little overlap of presynaptic (red) and postsynaptic (green) markers (arrow). ***B***, In contrast to E17, P5 neurons with astrocyte feeding layers show numerous synaptic puncta as illustrated by overlap of red and green, presynaptic and postsynaptic markers (yellow; arrows). Quantification of colocalized synaptic puncta on E17 and P5 neurons shows nearly a 10-fold difference in the number of synaptic puncta formed by P5 neurons ($p < 0.05$, *t* test). ***C***, Whole-cell voltage-clamp recordings from E17 neurons show low levels of spontaneous synaptic activity (downward deflections). Whole-cell voltage-clamp recordings from P5 neurons show high rates of spontaneous synaptic activity. Scale bars: ***A***, ***B***, 25 μm. Calibration: ***C***, 100 pA, 100 ms.

fied neurons stained with the amacrine-specific marker VC1.1 (data not shown), the other main type of neuron present in E17 retinas. Together, these results indicate that the cells that we isolated from E17 retina are highly purified RGCs.

Embryonic RGCs have many fewer synapses than postnatal RGCs

Purified P5 RGCs are able to make numerous synaptic connections in response to soluble astrocyte signals. This effect has been characterized through the use of astrocyte feeding layers in which astrocytes are cultured on a porous membrane and placed over cultured neurons, allowing for the diffusion of soluble astrocyte signals in the absence of direct neuron–glia contact (Mauch et al., 2001; Nägler et al., 2001; Ullian et al., 2001; Christopherson et al., 2005) (supplemental Fig. 3, available at www.jneurosci.org as supplemental material). To determine whether E17 neurons are able to form functional synapses under these conditions, we recorded spontaneous synaptic activity from cultured E17 or P5 neurons (Fig. 1*C*). We found that, as expected, P5 neurons had high rates of spontaneous synaptic activity, displaying on average 100 ± 24 synaptic events/min, mean ± SEM. In contrast, E17 neurons displayed very low rates of spontaneous synaptic activity, ~50 times less activity than the P5 neurons (2 ± 1 events/min, mean ± SEM; $p < 0.05$, *t* test).

The lower level of spontaneous synaptic activity exhibited by E17 neurons might result from nonfunctional or decreased numbers of synapses. To quantify synapse number, we immunostained purified RGCs cultured with astrocyte feeding layers for presynaptic synaptotagmin and postsynaptic PSD-95. We previously found that these two synaptic markers colocalize when mature structural synapses are present between RGCs (Ullian et al., 2001). As expected, immunostaining of P5 neurons cultured with astrocyte feeding layers revealed numerous synaptic puncta along dendrites and in somas with clear colocalization of presynaptic and postsynaptic markers (Fig. 1*B*). In contrast, E17 neurons exhibited few such synaptic puncta under the same culture conditions (i.e., with astrocyte feeding layers) and even after 4 weeks in culture (Fig. 1*A*). Quantification of the number of colocalized synaptic puncta indicates that there is a nearly 10-fold increase in the number of synapses formed on pure P5 neurons compared with pure E17 neurons (P5, 32.5 ± 5.0; E17, 3.75 ± 0.5, colocalized puncta per cell, mean ± SEM; $p < 0.05$, *t* test).

E17 RGCs can form but not receive synapses

Do E17 RGCs exhibit few synapses because they cannot form synapses onto each other, because they cannot receive synapses from each other, or both? To distinguish between these possibilities, we cocultured neurons of different ages (here E17 and P5), repeating the "heterochronic" culture experiments of Fletcher et al. (1994). By culturing high-density E17 RGCs with low-density, dye-labeled P5 RGCs for 2 weeks (Fig. 2*A*), we were able to assess the ability of E17 RGCs to form synapses. Under these conditions, the majority of synaptic inputs onto P5 RGCs will be from the much higher-density E17 RGCs, allowing us to determine whether the E17 RGCs are capable of forming normal synapses. We found that the high-density E17 neurons formed numerous structural and functional synapses onto P5 neurons. Immunostaining cocultures of high-density E17 neurons and low-density P5 neurons revealed numerous synaptic puncta along the dendrites of the P5 neurons (Fig. 2*B–E*). The total number of synapses formed on P5 neurons, ~40 synapses per neuron, is similar to the total number found in pure cultures of P5 neurons, ~30 synapses per neuron (Fig. 2*G*, left), indicating that E17 neurons are as good as P5 neurons at forming synapses. These synapses were fully functional as assessed by the frequency and amplitude of spontaneous synaptic events [Fig. 2*F* (top), *G* (right)]. These data show that E17 RGCs are capable of forming synapses when allowed to contact more mature receptive neurons. Interestingly, we saw few synapses formed on E17 neurons under these conditions.

To investigate the synaptic receptivity of E17 RGCs, we performed another heterochronic experiment, this time coculturing low-density dye-labeled E17 RGCs with high-density P5 RGCs. Under these conditions, the majority of synaptic inputs onto the E17 RGCs will be from the P5 RGCs. These conditions allow us to assess the ability of the E17 RGCs to receive synapses from postnatal RGCs and serve as a measure of synaptic receptivity, because postnatal RGCs are competent to form synapses in response to astrocyte feeding layers. Under these conditions, few structural synapses were formed by the P5 neurons onto the E17 neurons, as judged by immunostaining (Fig. 2*G*, left). Similarly, few functional synapses onto the embryonic neurons could be detected by whole-cell patch-clamp recordings [Fig. 2*F* (bottom), *G* (right)] (7 ± 3 events/min, mean ± SEM). Thus, both E17 and P5 RGCs were able to robustly form functional synapses, but E17 RGCs, unlike their postnatal counterparts, exhibited little ability to receive synapses.

Synaptic receptivity of E17 RGCs is not determined by dendritic elaboration

We next investigated whether the inability of E17 RGCs to receive synapses was attributable to insufficient dendrite elaboration. Previous reports indicate that embryonic RGCs extend axons robustly but are relatively poor at growing dendrites, until induced to do so by amacrine contact at P0 (Goldberg et al., 2002). It is possible that E17 neurons receive few synapses simply because they do not extend numerous dendritic arbors and thus have less area to receive synapses (Fletcher et al., 1994; Withers et

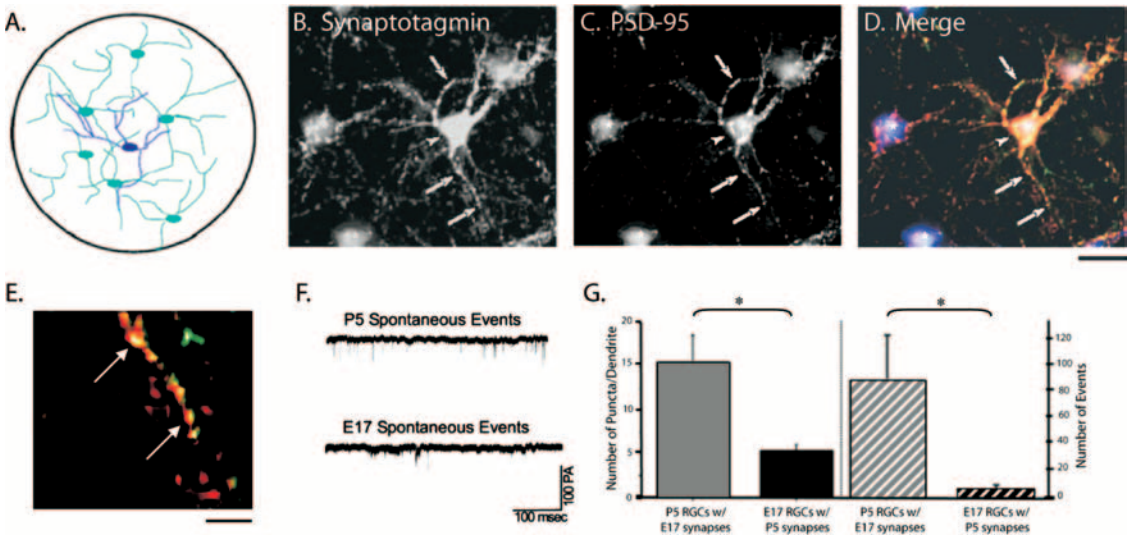

Figure 2. Heterochronic cocultures of labeled P5 neurons and E17 neurons. ***A***, Example of the culture technique: labeled P5 neurons (dark blue) are cocultured with unlabeled E17 neurons (turquoise), allowing for identification of the postnatal population. ***B–D***, P5 neuron (arrowhead) cocultured with E17 neurons (asterisks) and labeled for synaptotagmin (***B***; red in ***D***) and PSD-95 (***C***; green in ***D***). ***D***, The P5 neuron shows more synaptic staining and a greater colocalization of presynaptic and postsynaptic markers (arrows) than E17 neurons. ***E***, High magnification of P5 dendrite shown in ***D*** shows numerous synaptic puncta (yellow; arrows). ***F***, Spontaneous activity recorded with whole-cell patch clamp from P5 neurons shows numerous synaptic events (downward deflections; top). In contrast, recordings made from E17 neurons show fewer spontaneous synaptic events (bottom). ***G***, Left, Quantification of synaptic puncta per dendrite on E17 and P5 neurons in heterochronic culture conditions reveals a threefold increase in the number of synapses on P5 neurons compared with E17 neurons ($p < 0.001$, *t* test). Right, Quantification of the number of synaptic events shows a nearly 10-fold increase in the number of spontaneous events per minute recorded from P5 neurons with synapses from E17 neurons compared with synaptic events recorded from E17 neurons with synapses from P5 neurons. *$p < 0.05$. Scale bars: (in ***D***) ***B–D***, 50 μm; ***E***, 10 μm. Calibration: ***F***, 100 pA, 100 ms.

al., 2000). Interestingly, we found that we could induce substantial dendritic growth in E17 RGCs when cultured under astrocyte feeding layers for a prolonged culture period of 2 weeks, the same conditions used to quantify synapse formation. We labeled cocultured E17 and P5 neurons grown 2 weeks in culture with antibodies against the dendritic marker MAP2 (Fig. 3*A–C*). Detailed analysis revealed no statistically significant change in the number of primary dendrites on E17 and P5 neurons after 2 weeks in culture (Fig. 3*G*) ($p > 0.05$, *t* test). We further analyzed dendritic complexity by Sholl analysis and found no statistically significant difference in dendritic complexity between E17 and P5 neurons (Fig. 3*D–F*) ($p > 0.05$, *t* test).

To confirm that these E17 RGCs with long dendrites were not capable of receiving synapses, we immunostained the cocultures of labeled P5 RGCs and unlabeled E17 RGCs for MAP2 and synaptic markers and confirmed that the E17 RGCs were unable to receive many synaptic inputs along robust MAP2-positive dendrites (Fig. 4*A–F*). Therefore, the inability of E17 neurons to receive synapses cannot be explained by a lack of dendrites. Moreover, these data demonstrate that E17 RGCs do not acquire synaptic receptivity as a result of an intrinsic maturation program, because a prolonged 2 week culture period (one that mimics the age when all of the cells would have been synaptically receptive had they been left *in vivo*) does not result in synaptic receptivity.

Onset of synaptic receptivity requires contact with retinal cell types

RGCs begin to contact other cell types during the later stages of embryonic development. Although E17 neurons do not form many synapses as described previously, by E19, RGCs are capable of forming numerous synapses *in vitro* (E19, 27.5 ± 3.2; P5, 30.7 ± 4.7 colocalized synaptic puncta/cell; $p < 0.05$, Kruskal–Wallis ANOVA). These data indicate that although RGCs exhibit little synaptic receptivity at E17, they have rapidly acquired it by E19. Because E17 RGCs do not acquire synaptic receptivity over time in culture and E19 RGCs maintain synaptic receptivity acquired *in vivo* for prolonged culture periods *in vitro* (i.e., 4 weeks; data not shown), this strongly suggests that the retinal and/or optic environment is responsible for inducing synaptic receptivity at E19. To test this hypothesis, we cocultured labeled E17 neurons with mixed retinal cells (isolated by dissociation of whole retina) for 14 d to assess synaptic receptivity. We found that the E17 neurons cultured with mixed retinal cells were able to receive numerous synaptic inputs as assessed by patch-clamp recording of spontaneous synaptic currents (Fig. 5*A*,*B*) and by immunostaining (Fig. 5*D*,*F*). This switch did not occur when the RGCs were placed below a feeding layer of mixed retinal cells, but only when they were in direct contact with them (Fig. 5*A*,*B*). These results indicate that the retina provides a contact-mediated signal that induces synaptic receptivity in embryonic RGCs.

Astrocyte contact, but not amacrine contact, induces synaptic receptivity in RGCs

In retina, there are three cell types in the vicinity of the RGCs at the onset of synaptic receptivity (E19): cones, amacrine cells, and astrocytes (both in the retinal optic nerve fiber layer and optic nerve). Of these three, we can highly purify and culture amacrines and astrocytes. Because amacrine cells provide a major synaptic input onto RGCs, we first tested whether their presence would be sufficient to induce synaptic receptivity. We cocultured E17 RGCs in contact with purified amacrine cells and then determined the number of structural and functional synapses after 14 d of coculture. When we recorded from E17 RGCs cultured with amacrine cells, we did not find an increase in spontaneous excitatory synaptic events with patch-clamp recordings, even when cultured with a feeding layer of astrocytes (Fig. 5*A*,*B*). We also did not find an increase in the number of structural synapses when we immunostained these cultures for synaptic markers (Fig. 5*C*,*E*). These results indicate that amacrine cells, despite

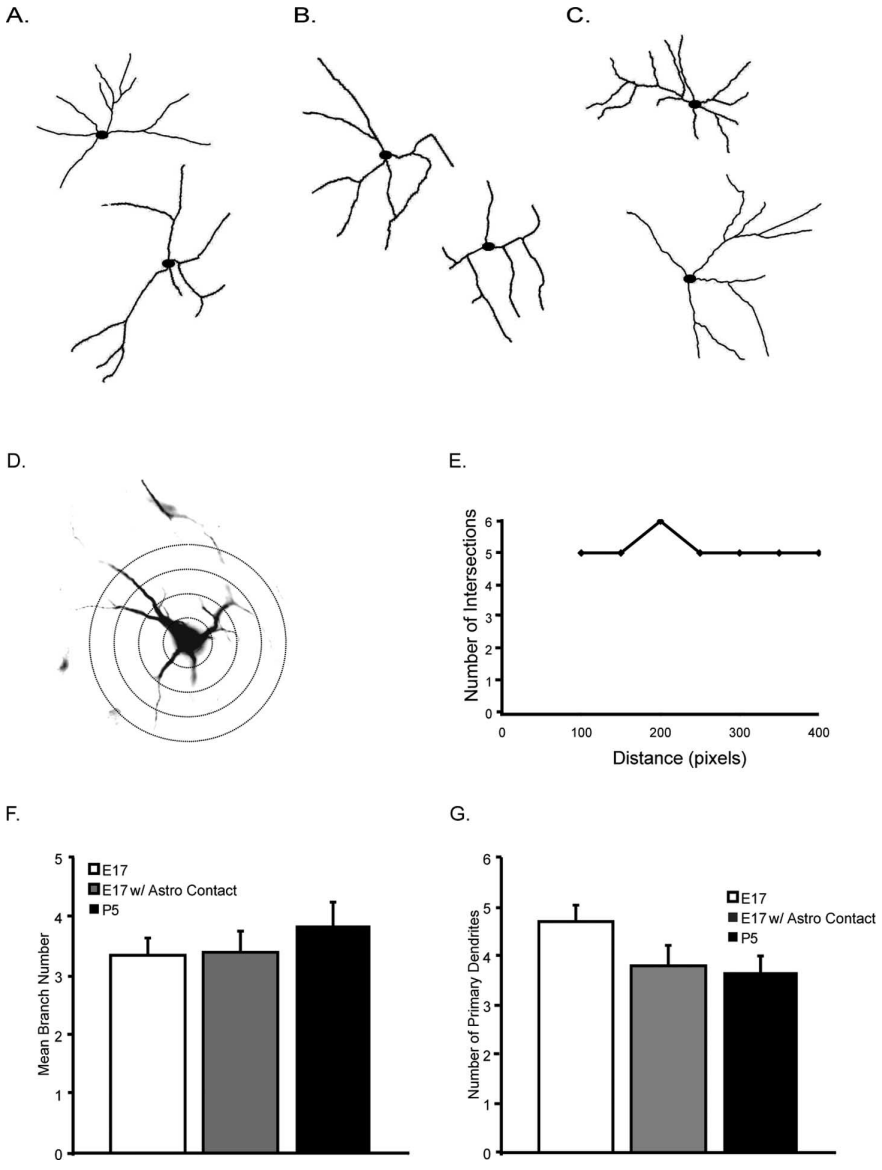

Figure 3. E17 and P5 neurons exhibit equivalent dendrite elaboration as illustrated by representative traces. ***A***, E17 RGCs. ***B***, E17 RGCs with direct astrocyte contact. ***C***, P5 RGCs. ***D***, Sholl analysis was used to quantify dendritic complexity. ***E***, Representative Sholl analysis for neuron shown in ***D***. ***F***, Sholl analysis was further used to quantify mean dendritic branch number. ***G***, Number of primary dendrites was also analyzed using Sholl analysis. No statistically significant difference was found between any of the three conditions. Astro, Astrocyte.

their strong dendrite-inducing ability (Goldberg et al., 2002), do not provide the signal for receptivity in E17 neurons.

Astrocyte precursor cells invade the retina from the optic nerve beginning around E17, and numerous astrocytes have migrated into the ganglion cell layer of the retina by E19 (Huxlin et al., 1992; Johnson et al., 1997). Furthermore, astrocyte precursor cells within the optic nerve do not differentiate into astrocytes until E19 (Mi and Barres, 1999), nearly the same time as the observed *in vitro* switch in synaptic receptivity. To determine whether astrocytes can provide a contact-mediated induction of synaptic receptivity in E17 RGCs, we cocultured E17 RGCs with purified optic nerve astrocytes for 14 d (supplemental Fig. 3, available at www.jneurosci.org as supplemental material). We found that under these culture conditions, E17 RGCs received numerous synapses as measured by immunostaining for synaptic markers (Fig. 5*G*,*I*). Quantification of synaptic puncta on E17 RGCs grown in contact with astrocytes indicates that astrocyte contact increases synapse number 10-fold (1.8 ± 0.5 no astrocyte contact vs 17.9 ± 1.4 astrocyte contact; $p = 0.009$). When compared with conditions of direct contact with amacrine cells, synaptic puncta on E17 RGCs increased nearly ninefold when cultured in direct contact with mixed retinal cells (1.36 ± 0.41; 11.7 ± 2.23; $p = 0.005$) and 19-fold when cultured in direct contact with astrocytes (1.36 ± 0.41; 26.5 ± 2.49; $p = 0.00012$) (Fig. 5*H*). Patch-clamp recordings revealed a large increase in spontaneous synaptic currents, indicating that the synapses formed in culture are fully functional (average peak amplitude was −56.7 ± 6.3 pA, and the average frequency was 3.5 ± 0.7 Hz) (Fig. 5*J*). These results indicate that astrocytes provide a contact-mediated signal allowing E17 neurons to receive synapses. We next asked whether the contact-mediated effect requires signaling from live cells or is preserved in fixed astrocyte membranes. We fixed live beds of astrocytes with methanol (100%), washed the fixed cells with DPBS, and plated labeled E17 RGCs on the astrocyte membranes and cultured them for 14 d. Under these conditions, we saw a slight fourfold increase in synapse number (1.75 ± 0.5 no contact vs 9.2 ± 0.9 fixed astrocyte contact; $p = 0.009$), indicating that a portion of activity is preserved in fixed membranes. We next wondered whether contact with astrocyte membranes could induce a switch in the ability of E17 neurons to respond to TSP. TSP is an extracellular matrix protein previously shown to be a soluble astrocyte-secreted factor competent to induce structural synapse formation (Christopherson et al., 2005). We fixed both astrocytes and amacrines from postnatal day 5 Sprague Dawley rats and plated E17 RGCs on each. Even with the repeated addition of TSP over a 2 week culture period, synapse formation was not significantly different between E17 neurons cultured on fixed astrocytes with and without TSP treatment (data not shown; 14% increase in synapses over control; $p = 0.21$), indicating that induction of synaptic receptivity by astrocyte contact is mechanistically distinct from the increase in synapse number caused by TSP.

In addition, astrocyte contact did not induce significant changes in E17 dendritic morphology as assessed by Sholl analysis (Fig. 3), indicating that astrocyte contact increases synaptogenesis independently of dendrite outgrowth.

Astrocyte contact has been found to increase synapse number on embryonic hippocampal neurons in a PKC-dependent manner (Hama et al., 2004). Is this mechanism conserved in retinal ganglion cells? We tested the necessity and sufficiency of PKC signaling in increasing synapse number in embryonic RGCs. E17 neurons treated with activators of the PKC signaling pathway did

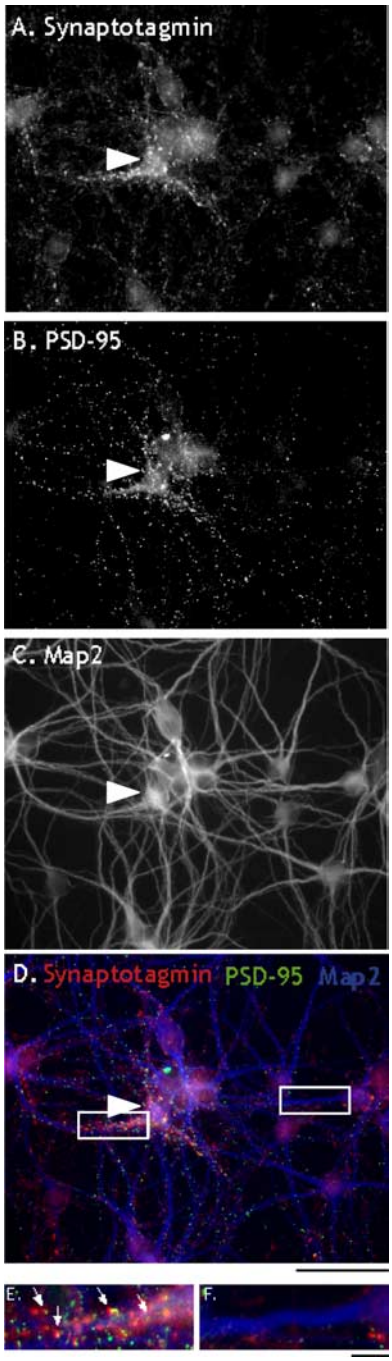

Figure 4. E17 neurons do not receive many synapses despite the presence of elongated dendrites in heterochronic cultures. ***A***, ***B***, Heterochronic E17 and P5 neuron culture stained for presynaptic marker, synaptotagmin (***A***), and postsynaptic marker, PSD-95 (***B***). Most synaptic puncta are associated with the P5 neuron (arrowhead). Few puncta are visibly associated with E17 neurons. ***C***, Dendritic staining shown in the same field as ***A*** and ***B***. Both P5 and E17 neurons contain numerous dendrites. ***D***, Triple label of presynaptic marker synaptotagmin (red), postsynaptic marker PSD-95 (green), and dendritic marker MAP2 (blue). Most colocalized puncta are found on P5 dendrites. ***E***, Detail of synaptic staining along dendrite of P5 neuron showing colocalization of presynaptic and postsynaptic markers (arrows). ***F***, Detail of synaptic staining along E17 dendrite. Few colocalized synaptic puncta are visible along the dendrite. Scale bars: (in ***D***) ***A–D***, 50 μm; (in ***F***) ***E***, ***F***, 10 μm.

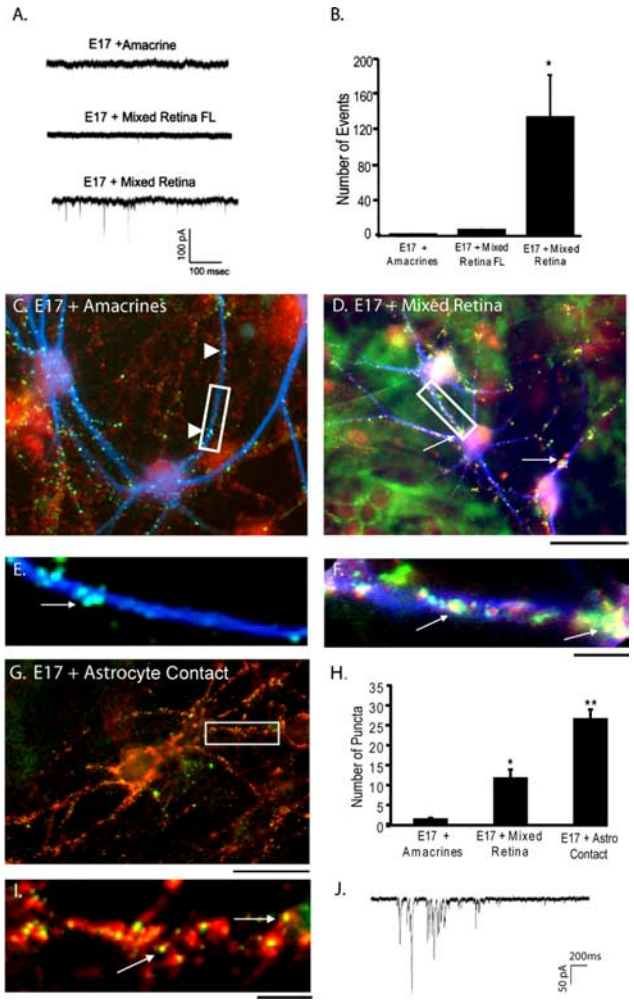

Figure 5. Mixed retinal cells, but not purified amacrine cells, increase spontaneous synaptic activity and synapse number on E17 neurons. ***A***, Patch-clamp recordings from E17 RGCs show few spontaneous events in neurons cocultured with amacrine cells (top), but numerous synaptic events in neurons cocultured with mixed retinal cells (bottom). E17 neurons cultured beneath mixed retinal feeding layers (Mixed Retina FL) also exhibit few spontaneous events (middle). ***B***, Quantification of spontaneous events reveals a >100-fold increase in synaptic events for neurons cultured with mixed retina compared with amacrine cells. *$p < 0.05$. ***C***, Immunostaining for synaptic puncta (arrowheads) with synaptotagmin (red) and PSD-95 (green) shows few colocalized puncta (white) on E17 neurons cocultured with amacrine cells. Dendrites are stained with MAP2 (blue). ***D***, Increased number of synaptic puncta (white; arrows) is observed on E17 neurons cocultured with mixed retina. Dendrites are stained with MAP2 (blue). Neurons are plated on top of a confluent layer of mixed retinal cells. ***E***, Detail of synaptic staining as shown in ***C***. Few colocalized puncta (white) are visible along the dendrite. ***F***, Detail of synaptic staining as shown in ***D***. Increases in colocalized puncta are observed. ***G***, E17 neurons cultured in contact with astrocytes (Astros) show an increase in the number of colocalized synaptic puncta (yellow) stained for synaptotagmin (red) and PSD-95 (green). Neurons are plated on top of a confluent monolayer of astrocytes. ***H***, Quantification of synaptic puncta reveals a ninefold increase in puncta when E17 RGCs are cultured on mixed retinal cells compared with amacrines and a 19-fold increase when cultured on astrocytes compared with amacrines. *$p < 0.05$; **$p < 0.0005$. ***I***, High-power image of colocalized puncta (yellow; arrows) on E17 neurons with astrocyte contact. ***J***, E17 neurons cocultured with astrocytes show marked increases in spontaneous synaptic currents as measured by whole-cell patch-clamp recording. Calibration: ***A***, 100 pA, 100 ms; ***J***, 50 pA, 200 ms. Scale bars: (in ***D***, ***G***) ***C***, ***D***, ***G***, 50 μm; (in ***F***, ***I***) ***E***, ***F***, ***I***, 10 μm.

not show an increase in synaptic puncta (data not shown), and blocking PKC signaling did not significantly interfere with the ability of astrocyte contact to increase synapse number on E17 neurons [17.9 ± 1.4 astrocyte contact vs 23.7 ± 2.5 astrocyte contact + GFX (an inhibitor of PKC action); $p > 0.05$]. Thus, unlike for hippocampal neurons, the PKC signaling pathway does not appear to be sufficient or necessary for astrocyte contact-mediated increases in synapse number in developing RGCs.

The astrocyte contact-dependent induction of synaptic recep-

tivity also does not depend on synaptic activity. We cultured E17 RGCs on astrocytes in the presence and absence of TTX and CNQX to block all synaptic transmission [all spontaneous synaptic transmission is mediated by AMPA receptors (Ullian et al., 2004b)]. Under these conditions, we found no difference in the number of synaptic puncta or in the frequency of spontaneous mEPSCs between the treated and untreated control cultures, indicating that synapse formation is not activity dependent.

We next asked, what is the exact relationship between the appearance of astrocytes in the retina and synaptogenesis? We immunostained E16, E19, E21, and P4 retinas for neuronal and astrocyte markers. Previous studies have reported astrocytes migrating into the retina around E18–E19 (Huxlin et al., 1992; Johnson et al., 1997; Mi and Barres, 1999). Similarly, we found evidence for GFAP-positive astrocytes in E19 retina (supplemental Fig. 2*A–F*, available at www.jneurosci.org as supplemental material). We next investigated the appearance of synaptic markers in the retina. Ultrastructural synapses, with clear vesicle accumulation and synaptic densities, first appear around P3 (Olney, 1968), but before this numerous contacts are made in the retina as synapses begin to form. To visualize the development of these contacts, we labeled RGCs and their dendrites with β-tubulin and innervating axons with SV2. We found that at E16–E17, there were very few SV2 puncta associated with RGCs, indicating that very few synaptic contacts have begun to form (supplemental Fig. 2*G–J*, available at www.jneurosci.org as supplemental material). By E19, however, we found a dramatic increase in the accumulation of SV2 immunoreactivity from the synaptic layer onto RGCs (supplemental Fig. 2*K–N*, available at www.jneurosci.org as supplemental material). The accumulating SV2 is both increasingly punctate and intense, with distinct puncta visible from E21 (supplemental Fig. 2*O–R*, available at www.jneurosci.org as supplemental material) to P4 (supplemental Fig. 2*S–V*, available at www.jneurosci.org as supplemental material), in line with the time course of ultrastructural synapse formation in the retina. Thus, the acquisition of synaptic receptivity by E19 RGCs temporally matches both the appearance of astrocytes and the formation of synapses *in vivo*.

Finally, we asked what potential mechanisms could contribute to the regulation of synaptic receptivity in embryonic neurons. To answer this question, we used immunostaining to screen embryonic neurons cultured with and without astrocyte contact for adhesion molecules involved in synaptogenesis. We analyzed the localization of numerous proteins, including N-cadherin, β-catenin, neuroligin, and neurexin. Most of these markers were localized in dendrites and changed from a diffuse to a punctuate pattern of staining consistent with their reported changes after synapse formation (Benson and Tanaka, 1998, Song et al., 1999, Taniguchi et al., 2007). Neurexin, however, dramatically changed from high dendritic localization to low dendritic localization in E17 neurons after contact with astrocytes (Fig. 6*A*,*C*). E17 neurons cultured in the absence of astrocyte contact displayed robust neurexin staining in dendrites (Fig. 6*A*,*D*). In contrast, E17 neurons cultured in contact with astrocytes showed a threefold reduction in neurexin immunoreactivity in dendritic compartments (Fig. 6*C*,*F*,*H*). Interestingly, the reduction in neurexin dendritic localization does not occur in response to the soluble astrocyte signal, TSP (Fig. 6*B*,*E*,*H*). This result suggests that astrocyte contact provides signals that both reduce dendritic neurexin and confer synaptic receptivity. We next wondered whether dendritic expression of neurexin in embryonic neurons might account for their reduced synaptogenic ability compared with P5 neurons. In P5 RGCs, neurexin immunoreactivity is reduced in dendrites compared with E17 (Fig. 6*G*) (P5, 48.2 ± 4.8 vs E17, 64.9 ± 4.1, mean grayscale value/12.5 μm length of dendrite, mean ± SEM; $p = 0.027$). Neuroligin, however, remained in dendritic compartments under all conditions and changed from a diffuse localization in E17 neurons without astrocyte contact to a highly punctate localization in E17 neurons with astrocyte contact, consistent with the reported changes associated with synapse formation (Fig. 6*I–L*).

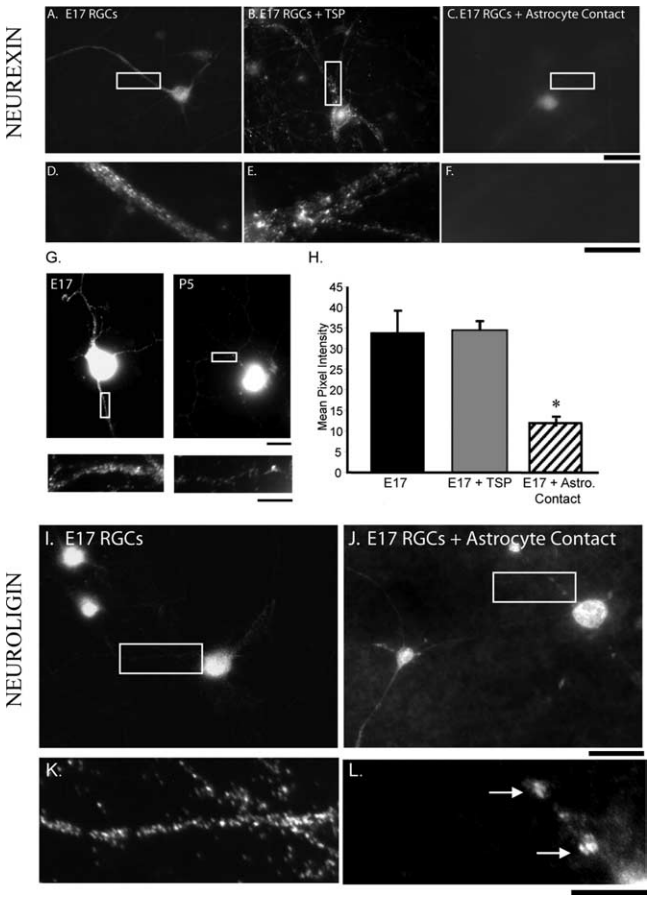

Figure 6. Astrocyte contact induces changes in localization and intensity of the synaptic proteins neurexin and neuroligin in E17 RGCs. ***A***, Neurexin staining of E17 RGCs cultured without astrocyte contact. ***B***, Neurexin staining of E17 RGCs treated with TSP. ***C***, Neurexin staining of E17 RGCs in contact with astrocytes. Intensity of neurexin staining decreases in E17 RGC dendrites when cultured on astrocytes but not with TSP treatment. ***D***, Detail of neurexin staining shown in ***A***. ***E***, Detail of neurexin staining shown in ***B***. ***F***, Detail of neurexin staining shown in ***C***. Quantification shows a significant decrease in intensity of neurexin staining (***H***). ***G***, Intensity of dendritic neurexin localization decreases in P5 RGCs compared with E17 RGCs. Left, Neurexin staining in E17 RGCs and high magnification of dendrite. Right, Neurexin staining in P5 RGCs and high magnification of dendrite. ***H***, Quantification of the intensity of neurexin staining shows a significant reduction when E17 RGCs are cultured in direct contact with astrocytes but not under conditions of TSP treatment. $^*p < 0.05$. Astro, Astrocyte. ***I***, E17 RGCs cultured without astrocyte contact exhibit diffuse neuroligin staining along dendrites. ***J***, When cultured in contact with astrocytes, neuroligin staining becomes punctate along dendrites. ***K***, Detail of neuroligin staining shown in ***I***. ***L***, Detail of neuroligin staining in E17 RGCs on astrocytes shown in ***J***, showing large puncta (arrows). Scale bars: (in ***C***, ***J***) ***A–C***, ***I***, ***J***, 50 μm; (in ***F***, ***L***) ***D–G***, ***K***, ***L***, 10 μm.

We were able to assess changes in the expression level of some NRX and NLG isoforms through the use of reverse transcription-PCR and Western blotting. When comparing retinal lysates from E17 and P5, we find a <3% reduction in protein levels of neurexin β-isoforms (supplemental Fig. 4*C*, available at www.jneurosci.org as supplemental material). During this same timeframe (E17 to P5), we note a large reduction in NRX1β mRNA

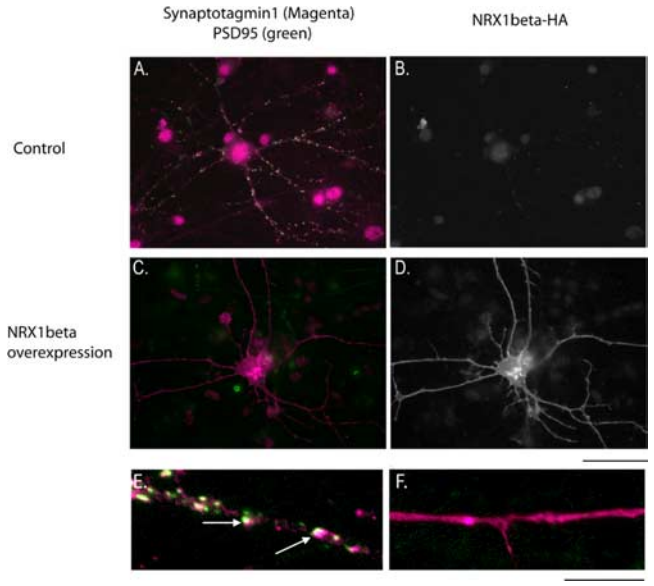

Figure 7. Overexpression of NRX1β greatly reduces the synaptogenic effects of astrocyte contact on embryonic RGCs. Embryonic neurons are plated on top of a confluent monolayer of astrocytes. ***A***, E17 RGCs cocultured with astrocytes exhibit many synaptic puncta. ***C***, E17 RGCs cocultured with astrocytes and transfected with an HA-tagged NRX1β construct exhibit few synapses. ***B***, ***D***, Transfection of the HA-tagged NRX1β construct is visualized by staining for the HA tag. ***E***, ***F***, High-magnification images of untransfected E17 RGCs (***E***) and NRX1β-transfected E17 RGCs (***F***) highlight the large reduction in synapse number when NRX1β is overexpressed (synaptic puncta denoted by arrows). Quantification of synapse number reveals a highly significant reduction ($p < 0.000005$, Student's *t* test). Scale bars: (in ***D***) ***A–D***, 50 μm; (in ***F***) ***E***, ***F***, 10 μm.

(supplemental Fig. 4*A*, available at www.jneurosci.org as supplemental material) (84%) and an increase in NRX2β mRNA (supplemental Fig. 4*A*, available at www.jneurosci.org as supplemental material) (70%). mRNA levels of NLG1 appear to increase slightly during this timeframe (supplemental Fig. 4*B*, available at www.jneurosci.org as supplemental material) (23%). Interestingly, postsynaptic neurexin expression has been reported to reduce synapses (Taniguchi et al., 2007), raising the possibility that postsynaptic neurexin expression is a mechanism used by developing neurons to regulate the timing of synapse formation. If astrocyte contact mediates synaptic receptivity in part by redistributing neurexin, we predict persistent dendritic expression of neurexin will attenuate synaptic receptivity resulting from contact between astrocytes and developing neurons. Indeed, we find that dendritic expression of an HA-tagged neurexin1 β isoform in E17 RGCs cultured on astrocytes blocks the induction of synaptic receptivity in these neurons (Fig. 7*A–F*) (control, 58.5 $\pm$ 6.62; HA transfected, 10.2 $\pm$ 2.37 colocalized puncta per cell, mean $\pm$ SEM; $p = 0.000004$).

Discussion

Newly generated RGCs can form synapses onto more mature neurons but are not competent to receive them

Although it was generally thought that neurons in the developing brain were generated with the ability to both form and receive synapses, elegant studies by Fletcher et al. (1994) and Withers et al. (2000) have shown that axons and dendrites of embryonic hippocampal neurons in culture became competent for synaptogenesis at different stages of development. In these studies, hippocampal neurons developed a significant number of synapses, as measured by immunostaining, concurrent with their elaboration of dendrites or in response to BMP-7 stimulation. These studies suggested that a dendrite maturation dependent program controlled the acquisition of synaptic receptivity by controlling the timing of dendritic arborization.

Our findings add to the understanding of how newly formed neurons in the developing CNS acquire competence to receive synapses by demonstrating that two distinct mechanisms are present, one determining dendrite elaboration and a second controlling synaptic receptivity. By studying the ability of highly purified RGCs in culture to both form and receive synapses, we found that RGCs from the earliest stage that we could purify them, E17, were capable of forming synapses onto more mature neurons (here P5 neurons), and were induced by other cell types to become competent to receive synapses at E19. RGCs under the age of E19 were unable to receive synapses even when cultured for several weeks, suggesting that receptivity is not attributable to a purely intrinsic mechanism. Thus, synaptic receptivity appears during a short window of development, between embryonic days 17 and 19. We were able to clearly distinguish the acquisition of synaptic receptivity from the generation and elaboration of dendrites. Remarkably, E17 RGCs after 2 weeks in culture with astrocyte feeding layers elaborate long dendrites, yet continue to be synaptically unreceptive. Because their axons are able to form synapses without difficulty, these findings point to the existence of an as yet unidentified postsynaptic mechanism in E17 RGCs that controls their synaptic receptivity. This mechanism might be accounted for either by the presence of a molecule that inhibits synaptogenesis or the absence of a molecule necessary for synaptogenesis (with synaptogenesis defined as any mechanism that increases synapse number by enhancing the rate of synapse formation or synaptic stability). Our evidence provides support for the former.

Competence to receive synapses is induced by extrinsic signals from neighboring retinal or optic nerve cells and by direct contact with retinal astrocytes

How is competence to receive synapses acquired by RGCs at E19? Our findings show that it does not occur as the result of an age-dependent intrinsic mechanism and that dendrite formation and elaboration are also insufficient. Rather, we found that contact-mediated signals from other retinal and optic nerve cell types are sufficient to induce synaptic receptivity. This change is reminiscent of, but mechanistically distinct from, a similar change we have previously identified at P0 in RGCs. We found that embryonic RGCs are capable of extending axons rapidly but dendrites slowly, whereas at P0 they lose the intrinsic ability to extend their axons rapidly but gain the ability to rapidly elaborate dendrites. This change is triggered by amacrine contact abruptly at P0 and is apparently irreversible (Goldberg et al., 2002). In contrast, here we found that embryonic neurons are not competent to receive synapses but abruptly acquire this competence at E19, and that here amacrine cells are not able to induce this switch.

Our findings indicate that once an RGC has been generated from a progenitor cell, it does not yet contain all the properties of a fully functional neuron, but must be signaled through a series of cell–cell interactions to become fully mature. In particular, they raise the question, how is the acquisition of competence for synaptic receptivity signaled? Possible cell types that could provide this signal *in vivo* include afferent inputs onto the neuron, target contact by RGC axons, or contact by glial cells within the retina, optic nerve fiber layer, or along the optic nerve. Our initial results showed that direct contact with mixed retinal cells was sufficient to induce synaptic receptivity, helping to focus our search. The two most relevant retinal neurons with potential synaptic inputs onto RGCs at E19 are amacrine cells and cone photoreceptors

(Wong et al., 1992; Lohmann et al., 2002). Other retinal neurons that might synapse onto RGCs, such as bipolar neurons, are largely generated after E19. We were unable to purify the cone photoreceptors, but were able to directly test the possible effects of amacrine cells by purifying them and coculturing them with E17 RGCs. We found they were insufficient to induce synaptic receptivity, despite their ability to greatly enhance dendritic elaboration.

Glial cells make extensive direct contact with RGCs at E19, both the Müller glia within the retina and astrocytes within the retinal optic nerve fiber layer and optic nerve. Few Müller glia are generated by E19; however, astrocyte precursor cells are extensively differentiating into astrocytes in both the retina and optic nerve (Huxlin et al., 1992; Johnson et al., 1997; Mi and Barres, 1999) at E19, occurring almost exactly with the switch in synaptic receptivity. We found that coculture of E17 RGCs in direct contact with optic nerve astrocytes was sufficient to induce the RGCs to acquire synaptic receptivity. These results implicate astrocyte contact as a likely inducer of synaptic receptivity, but it remains to be determined whether other retinal cell types might also contribute.

Support for the notion that astrocytes provide the *in vivo* signal for synaptic receptivity comes from observations of the timing of astrocyte ingrowth to the retina and the beginnings of synapse formation. We found that the first GFAP-positive astrocytes appear at the time of the switch in synaptic receptivity (E19), and this corresponds to synaptic vesicle accumulation in the retinal synaptic layer of the RGCs, beginning at E19 and continuing until bona fide synapses are first detected at P3 (supplemental Fig. 2, available at www.jneurosci.org as supplemental material) (Olney, 1968). Thus, the formation of synapses *in vivo* supports our findings of the development of synaptic receptivity *in vitro*, and strongly implicates astrocytes as one component of the developmental switch.

Recently, embryonic hippocampal neurons have also been found to be induced to form synapses by astrocyte contact. In this case, astrocyte contact leads to an integrin-dependent activation of PKC that in turn leads to global synapse formation (Hama et al., 2004). It is not clear from these studies, however, if this represents a switch in the ability of hippocampal neurons to make or receive synapses, because the study used autaptic cultures. Our findings add to the understanding of synapse formation by showing that (1) newly generated neurons are not fully competent to receive synapses but must be signaled during development to do so, (2) dendrite outgrowth is mechanistically distinct from synaptic receptivity, and (3) astrocytes provide a contact-mediated signal(s) that can at least in part induce the switch to receptivity.

Astrocytes promote synapse formation by at least two mechanisms

Together with previous studies (Pfrieger and Barres, 1997; Nägler et al., 2001; Mauch et al., 2001; Ullian et al., 2001; Song et al., 2002a,b), the present findings indicate that astrocytes induce synaptogenesis by at least two different mechanisms. First, they induce the acquisition of competence for synaptic receptivity. This effect requires direct contact of the astrocytes with RGCs. Second, astrocytes release soluble signals such as thrombospondin that greatly increase synapse number. This effect is highly reversible, because these astrocyte-derived soluble signals are necessary for synaptic maintenance (Ullian et al., 2001).

Despite these differences, are these two mechanisms by which astrocytes induce synapses nonetheless related? One simple possibility is that the receptors for the soluble synapse-inducing proteins secreted by astrocytes are induced in the RGCs, or directed to their dendrites, by direct astrocyte contact. Another possibility is that the receptors are constitutively present in the dendrites but are functionally inhibited or inaccessible before astrocyte contact. Astrocyte contact most likely induces synaptic receptivity by acting postsynaptically, because the E17 RGCs are able to form synapses without difficulty onto the dendrites of more mature neurons. One possible mechanism by which astrocyte contact regulates the timing of synaptic receptivity is by altering the localization of neurexin. We found that neurexin immunoreactivity is high on E17 dendrites without astrocyte contact, and this immunoreactivity is dramatically reduced in E17 neurons in contact with astrocytes. Recently, it has been reported that neurexin is expressed at low levels at postsynaptic sites in more mature hippocampal neurons and that increasing postsynaptic expression of neurexin can reduce synapse number. Thus, the number or timing of synapse formation may be regulated by regulating the levels of postsynaptic neurexin expression (Taniguchi et al., 2007). Our findings extend this observation by showing that neurons purified from early retina continue to exhibit high levels of diffuse dendritic neurexin, whereas neurons purified from postnatal retina have reduced localization of neurexin in their dendrites, suggesting that mechanisms controlling the expression or localization of neurexin can change in neurons. Previous studies have demonstrated the differential expression patterns of the three neurexin genes both in the adult and developing brain (Ushkaryov et al., 1992, Ullrich et al., 1995, Püschel and Betz, 1995). More recent studies show an upregulation of specific neurexin transcripts in response to insult (Górecki et al., 1999; Sun et al., 2000). It is of interest to note that mRNA levels of NRX1β are reduced from E17 to P5 in retina, whereas another neurexin gene β-isoform (NRX2β) shows increased levels of transcription during this time. Although we cannot definitely localize these changes to retinal ganglion cell dendrites, further experiments may show neuronal compartment or developmental specificity for the neurexin family members, perhaps as a means of fine-tuning the positioning and timing of synaptogenesis. Finally, we are able to block astrocyte-induced synaptic receptivity in embryonic neurons by expressing high levels of neurexin dendritically. We find that dendritic overexpression of the β-isoform of a single neurexin gene (NRX1) is sufficient to attenuate astrocyte contact-mediated effects on synaptic receptivity, extending our understanding of potential mechanisms by which astrocyte contact influences the developing dendrite. The present findings that astrocytes can induce synapse formation by inducing competence for synaptic receptivity independently of dendrite outgrowth expand our understanding of synaptic circuit formation and add to the rapidly growing body of evidence that astrocytes are highly specialized to support, regulate, and control synaptic function and plasticity.

References

Barres BA, Silverstein BE, Corey DP, Chun LL (1988) Immunological, morphological, and electrophysiological variation among retinal ganglion cells purified by panning. Neuron 1:791–803.

Benson DL, Tanaka H (1998) N-cadherin redistribution during synaptogenesis in hippocampal neurons. J Neurosci 18:6892–6904.

Bottenstein J, Hayashi I, Hutchings S, Masui H, Mather J, McClure DB, Ohasa S, Rizzino A, Sato G, Serrero G, Wolfe R, Wu R (1979) The growth of cells in serum-free hormone-supplemented media. Methods Enzymol 58:94–109.

Christopherson KS, Ullian EM, Stokes CC, Mullowney CE, Hell JW, Agah A, Lawler J, Mosher DF, Bornstein P, Barres BA (2005) Thrombospondins are astrocyte-derived proteins that promote CNS synaptogenesis. Cell 120:421–433.

Craig AM, Kang Y (2007) Neurexin-neuroligin signaling in synapse development. Curr Opin Neurobiol 17:43–52.

Dean C, Dresbach T (2006) Neuroligins and neurexins: linking cell adhesion, synapse formation and cognitive function. Trends Neurosci 29:21–29.

Fletcher TL, De Camilli P, Banker G (1994) Synaptogenesis in hippocampal cultures: evidence indicating that axons and dendrites become competent to form synapses at different stages of neuronal development. J Neurosci 14:6695–6706.

Goldberg JL, Klassen MP, Hua Y, Barres BA (2002) Amacrine-signaled loss of intrinsic axon growth ability by retinal ganglion cells. Science 296:1860–1864.

Górecki DC, Szklarczyk A, Łukasiuk K, Kaczmarek L, Simons JP (1999) Differential seizure-induced and developmental changes of neurexin expression. Mol Cell Neurosci 13:218–227.

Hama H, Hara C, Yamaguchi K, Miyawaki A (2004) PKC signaling mediates global enhancement of excitatory synaptogenesis in neurons triggered by local contact with astrocytes. Neuron 41:405–415.

Huxlin KR, Sefton AJ, Furby JH (1992) The origin and development of retinal astrocytes in the mouse. J Neurocytol 21:530–544.

Johnson PT, Geller SF, Lewis GP, Reese BE (1997) Cellular retinaldehyde binding protein in developing retinal astrocytes. Exp Eye Res 64:759–766.

Liu W, Khare SL, Liang X, Peters MA, Liu X, Cepko CL, Xiang M (2000) All Brn3 genes can promote retinal ganglion cell differentiation in the chick. Development 127:3237–3247.

Lohmann C, Myhr KL, Wong RO (2002) Transmitter-evoked local calcium release stabilizes developing dendrites. Nature 418:177–181.

Mauch DH, Nägler K, Schumacher S, Göritz C, Müller EC, Otto A, Pfrieger FW (2001) CNS synaptogenesis promoted by glia-derived cholesterol. Science 294:1354–1357.

McCarthy KD, de Vellis J (1980) Preparation of separate astroglial and oligodendroglial cell cultures from rat cerebral tissue. J Cell Biol 85:890–902.

Meijering E, Jacob M, Sarria JCF, Steiner P, Hirling H, Unser M (2004) Design and validation of a tool for neurite tracing and analysis in fluorescence microscopy images. Cytometry A 58:167–176.

Meyer-Franke A, Kaplan MR, Pfrieger FW, Barres BA (1995) Characterization of the signaling interactions that promote the survival and growth of developing retinal ganglion cells in culture. Neuron 15:805–819.

Mi H, Barres BA (1999) Purification and characterization of astrocyte precursor cells from the developing rat optic nerve. J Neurosci 19:1049–1061.

Nägler K, Mauch DH, Pfrieger FW (2001) Glia-derived signals induce synapse formation in neurons of the rat central nervous system. J Physiol 533:665–679.

Olney JW (1968) An electron microscopic study of synapse formation, receptor outer segment development, and other aspects of developing mouse retina. Invest Ophthalmol 7:250–268.

Pfrieger FW, Barres BA (1997) Synaptic efficacy enhanced by glial cells in vitro. Science 277:1684–1687.

Püschel AW, Betz H (1995) Neurexins are differentially expressed in the embryonic nervous system of mice. J Neurosci 15:2849–2856.

Song H, Stevens CF, Gage FH (2002a) Astroglia induce neurogenesis from adult neural stem cells. Nature 417:39–44.

Song HJ, Stevens CF, Gage FH (2002b) Neural stem cells from adult hippocampus develop essential properties of functional CNS neurons. Nat Neurosci 5:438–445.

Song JY, Ichtchenko K, Südhof TC, Brose N (1999) Neuroligin 1 is a postsynaptic cell-adhesion molecule of excitatory synapses. Proc Natl Acad Sci U S A 96:1100–1105.

Sun HB, Yokota H, Chi XX, Xu ZC (2000) Differential expression of neurexin mRNA in CA1 and CA3 hippocampal neurons in response to ischemic insult. Brain Res Mol Brain Res 84:146–149.

Taniguchi H, Gollan L, Scholl FG, Mahadomrongkul V, Dobler E, Limthong N, Peck M, Aoki C, Scheiffele P (2007) Silencing of neuroligin function by postsynaptic neurexins. J Neurosci 27:2815–2824.

Ullian EM, Sapperstein SK, Christopherson KS, Barres BA (2001) Control of synapse number by glia. Science 291:657–661.

Ullian EM, Harris BT, Wu A, Chan JR, Barres BA (2004a) Schwann cells and astrocytes induce synapse formation by spinal motor neurons in culture. Mol Cell Neurosci 25:241–251.

Ullian EM, Barkis WB, Chen S, Diamond JS, Barres BA (2004b) Invulnerability of retinal ganglion cells to NMDA excitotoxicity. Mol Cell Neurosci 26:544–557.

Ullrich B, Ushkaryov YA, Südhof TC (1995) Cartography of neurexins: more than 1000 isoforms generated by alternative splicing and expressed in distinct subsets of neurons. Neuron 14:497–507.

Ushkaryov YA, Petrenko AG, Geppert M, Südhof TC (1992) Neurexins: synaptic cell surface proteins related to the alpha-latrotoxin receptor and laminin. Science 257:50–56.

Watanabe M, Rutishauser U, Silver J (1991) Formation of the retinal ganglion cell and optic fiber layers. J Neurobiol 22:85–96.

Withers GS, Higgins D, Charette M, Banker G (2000) Bone morphogenetic protein-7 enhances dendritic growth and receptivity to innervation in cultured hippocampal neurons. Eur J Neurosci 12:106–116.

Wong RO, Yamawaki RM, Shatz CJ (1992) Synaptic contacts and the transient dendritic spines of developing retinal ganglion cells. Eur J Neurosci 4:1387–1397.